Electronic Supplementary Material (ESI) for Chemical Science.

Supporting Information

Unravelling the Carbonate Issue through the Regulation of the Mass Transport and Charge Transfer in Mild Acid

Zhongshuo Zhang, Qian Lu, Jiping Sun, Guangchao Li, Weixing Wu, Zhanyou Xu, Liangpang Xu, and Ying Wang*

*Correspondence and requests for materials should be addressed to Ying Wang (ying.b.wang@cuhk.edu.hk) (Y.W.)

Experimental Section

Materials

Potassium sulphate (K_2SO_4, ACS), lithium sulphate (Li_2SO_4, 99.9% metals basis) and potassium chloride (KCl, GR) were purchased from Shanghai Aladdin reagent co. Ltd. Sulfuric acid (H_2SO_4, AR, 98%) was purchased from RCl Labscan Ltd. Perchloric acid ($HClO_4$, ACS, 70%) is purchased from VWR Chemicals. Potassium perchlorate ($KClO_4$, 99+%) was purchased from International Laboratory USA. All the chemical reagents were used as received without any other purification. All aqueous solutions were prepared using deionized water with a resistivity of 18.25 MΩ cm. The acidified $KClO_4$ electrolyte was prepared by adding $HClO_4$ into $KClO_4$ solution. Other acidic electrolytes were prepared by adding H_2SO_4 into the salt solutions.

Electrode Preparation

For electrodes used in the DEMS test and pH dependency experiments, 18 mg of commercial 50 nm Ag nanoparticles (MG-Ag-50, Shanghai Maogon nanotechnology co. Ltd.) and 8 μL of perfluorosulfnic acid dispersion (Aquivion® D72-25BS) were dispersed in 2 mL H_2O and 4 mL Isopropanol. The mixture was sonicated for 1 h to obtain a uniform catalyst ink. The prepared ink was sprayed onto a piece of Sigracet 39BB carbon paper (6.5 cm × 6.5 cm). All samples were dried overnight before testing.

x%-PTFE/Ag electrodes were prepared on YLS30T substrate. The catalyst inks were prepared as follows. For 0%-PTFE/Ag electrode, 5.75 mg of commercial Ag nanoparticles (MG-Ag-50, Shanghai Maogon nanotechnology co. Ltd.), 0.58 mg of Vulcan XC 72 carbon black (Fuel Cell store) and 2.3 μL of perfluorosulfnic acid dispersion (Aquivion® D72-25BS) were dispersed in 0.64 mL H_2O and 1.29 mL Isopropanol. After sonication for 1h, the catalyst ink was

sprayed onto a piece of YLS30T substrate (1.5 cm × 5 cm). For 10 – 70%-PTFE/Ag electrodes, 5.75 mg of commercial Ag nanoparticles (MG-Ag-50, Shanghai Maogon nanotechnology co. Ltd.), 0.58 mg of Vulcan XC 72 carbon black (Fuel Cell store) and 2.3 μL of perfluorosulfnic acid dispersion (Aquivion® D72-25BS) were added to 0.43 mL H_2O and 0.86 mL isopropanol. Then, 0.77, 2.96, 6.91 and 16.12 mg of PTFE nanoparticle (APS 30-40 nm, Nanoshel LLC) was dispersed in 0.21 mL H_2O and 0.43 mL isopropanol, respectively. After sonication for 1h, the two dispersions were mixed and sonicated for another 1 h, which were used as 10%, 30%, 50% and 70% PTFE-catalyst inks. Each catalyst ink was sprayed onto a piece of YLS30T substrate (1.5 cm × 5 cm). For 10 – 70%-PTFE/Ag electrodes, an additional C layer was deposited on top as follows for uniform current distribution. 0.75 mg Vulcan XC 72 carbon black (Fuel Cell store) and 3 μL of perfluorosulfnic acid dispersion (Aquivion® D72-25BS) were added to 0.25 mL H_2O and 0.5 mL Isopropanol. The ink was sprayed onto Ag/10% – 70% PTFE electrode after sonication for 1 h. All samples were dried overnight before testing.

Characterization

The post-reaction cross section scanning electron microscopy (SEM) image was collected using Phenom Pro. The SEM images before and after electrolysis were collected using ZEISS Sigma 300. The X-ray diffraction (XRD) patterns were collected using Bruker D8 Venture. The X-ray photoelectron spectroscopy was collected using Thermo Scientific K-Alpha.

Electrochemical Measurements

Unless otherwise noted, electrochemical tests were performed using a Zahner instrument Zennium Pro potentiostat with a flow cell.

The flow cell experiments were carried out in an electrochemical flow cell electrolyzer with three-electrode configuration. Ag/AgCl electrode (saturated with KCl, IDA) and Pt mesh were used as reference and counter electrode, respectively. Electrodes with YLS30T substrate were used as the working electrode, and the area of the electrode exposed was 1.44 cm^2 ($1.2\ cm \times 1.2\ cm$). A proton exchange membrane (Nafion 117, Fuel Cell Store) was used to separate catholyte and anolyte chamber. The acidified K_2SO_4 or KCl was used as the catholyte and 0.5 M H_2SO_4 was used as the anolyte. The catholyte and anolyte were circulated through the cathode and anode chamber at different rates by two peristaltic pumps, respectively. Unless otherwise noted, CO_2 was continuously fed into the gas chamber at a fixed flow rate of 40 sccm, and the catholyte is flowed in the catholyte chamber at 13 sccm.

Products Analysis

Gaseous products were analyzed by gas chromatograph (Ramiin GC 2060) or Differential Electrochemical Mass Spectrometry.

Gas chromatograph (Ramiin GC 2060) is equipped with flame ionization and thermal conductivity detectors. The calibration curves for CO, CH_4, C_2H_4 and H_2 were obtained by injection of certified standard gas samples (Scientific Gas Engineering Co., Ltd.) diluted with pure CO_2.

FE for each product was calculated based on the following equation:

$$FE_i = \frac{z_i \times x_i \times F}{Q} \times 100\%$$

where z_i is the number of electrons transferred for product, x_i is the number of moles of the product, F is Faraday's constant, and Q is the total charge passed during electrolysis.

The single-pass carbon utilization efficiency (SPCE) was calculated based on the following equation:

$$SPCE = \frac{j_{CO} \times 60\ s/min \times 24000\ cm^3/mol}{z_i \times F \times v_{in}}$$

where j_{CO} is the partial current density of CO, and v_{in} is the gas supply rate.

In Differential Electrochemical Mass Spectrometry (DEMS), the gas products were detected by a PrismaPro quadrupole mass spectrometer (QMG 250 M3, Pfeiffer-Vacuum), with sampling time interval of 1 s. The cathode potential of the ion source is set to -27 V. The fragmentation of CO_2 for mass 28 is negligibly small at this cathode potential. The gases are ionized by the ion source in DEMS, which are then collected by the detector and generate ionic current (I_I). The magnitude of ionic current reflects formation rate of species *i* (I_I^i) according to the equation below.

$$I_I^i = K_i J_i$$

Where K_i is a constant containing all settings of DEMS and the ionization probability of the species *i*, and J_i is the incoming flux of species *i*.

The ionic current for mass 2 and 28 could be assigned to the produced H_2 and CO. For quantification of CO, the calibration curves for CO was obtained by flowing CO diluted with pure CO_2 into DEMS.

Determination of the diffusion layer thickness

The diffusion layer thickness was experimentally estimated by measuring the diffusion-limited current density of hydrogen evolution reaction (HER) by chronoamperometry. Considering that

our hydrodynamic conditions provide laminar flows based on the calculation of Reynold's number (Supplementary Table 4), we assumed that a uniform diffusion layer was established near the electrode surface in each case.[1] The concentration of H_3O^+ is determined by a pH meter. The diffusion-limited current density follows:

$$j_{lim} = \frac{nFD_{H_3O^+} c_{H_3O^+,\ bulk} + nFD_{HSO_4^-} c_{HSO_4^-,\ bulk}}{\delta}$$

where j_{lim} is the diffusion-limited current density; n is the number of electron transfer, F is the Faraday's constant, D is the diffusion coefficient, δ is the diffusion layer thickness.

The diffusion layer thickness can thus be estimated based on the following equation:

$$\delta = \frac{nFD_{H_3O^+} c_{H_3O^+,\ bulk} + nFD_{HSO_4^-} c_{HSO_4^-,\ bulk}}{j_{lim}}$$

The diffusion layer thickness at electrolyte flow rate of 13 – 63 sccm is shown in Supplementary Fig. 1.

Scanning Electrochemical Microscopy setup

All the Scanning Electrochemical Microscopy (SECM) experiments were performed with a CHI 900 setup (CH Instruments Inc, USA). An additional workstation (CHI 1101, CH Instruments Inc, USA) working in float mode was used to apply constant currents on the substrate. A 10 μm Pt ultramicroelectrode (Pt UME) was used as the tip and a Ag nanoparticles-modified glass carbon electrode was used as the substrate.

SECM approach curves were performed to place the tip close to the substrate with known distances. To avoid the addition of redox mediators in the electrolyte, we utilized dissolved O_2 as the reactive species for its easy removal after tip approach. The electrolyte was first saturated with O_2. The Pt tip was then placed at a cathodic potential (-0.23 V vs. Ag/AgCl) where oxygen

reduction reaction (ORR) is under mass transportation control. After the current reaches steady, the Pt tip was slowly approached to the electrode surface. Negative feedback on the current happens because of the hindered mass transportation of O_2. The obtained current was then fitted using the known parameters (tip radius = 5 μm, Rg = 5) to establish the current – distance relationship (Supplementary Fig. 3). The tip was adjusted to 50 μm above the substrate according to the ORR approach curve, and the electrolyte was then saturated with CO_2 to perform CO_2 reduction experiments.

An amperometric method was adopted for local pH measurement.[2] HER diffusion-limited current (DLC) was measured on the Pt tip, which is proportional to the proton concentration at the tip:

$$i = 4nFDca$$

where n is the number of electron transfer, which is 1 for H^+-HER; F is the Faradaic constant; D is the diffusion coefficient; c is the concentration of species at the tip; a is the radius of the tip.

The HER DLC on Pt surface is reported to be surface poison-resisting to CO,[2] which allows us to measure the local proton concentration near a CO-producing substrate. The HER DLC at 50 μm above the substrate was measured when a series of applied current densities were applied on the substrate. Under unbiased substrate, where consumption of local protons does not happen, the local pH is assumed equal to its bulk value 2. The increase in local pH could thus be calculated by comparing the HER DLC at biased and unbiased substrates (Supplementary Fig. 4). Every decade decrease in tip current corresponds to 1 unit of pH increase.

Multiphysics Modeling Methods

Overview

The simulation was conducted with COMSOL (COMSOL Multiphysics v5.4, Stockholm, Se). All the models were simulated as one-dimensional (1D) domains, including an electrode and a liquid diffusion layer (DL) located adjacent to the electrode. The thickness of DL was experimentally determined by the method mentioned in the experimental section. Charge transfer reaction of CO_2 reduction reaction (CO_2RR), acid-base carbonate equilibria, and dilute species transport physics in liquid phase were considered in all the models, as detailed below. The main difference in each model lies in the electrode part. For the planar electrode system, as adopted in the SECM experiments, the electrode surface was simulated as a point at the left boundary (x = 0 μm). For the flow cell system, a catalyst layer (CL) was simulated as a 0.5 μm-thick media with 60% porosity. In fully wetted GDE, only solid and liquid phases exist in the CL, corresponding to saturation value, S = 1. Solid, liquid and gas phases exist in the CL of partially wetted GDE. We assumed S = 0.64, based on the previously reported optimal value.[3]

Physics within the Multiphysics model

CO_2 solubility

The quantity of dissolved CO_2 in solution is determined by the temperature, pressure, and solution salinity. With the assumption that CO_2 is an ideal gas, the dissolved amount is given by Henry's Law:[4]

$$[CO_2]_{aq,0} = K_0[CO_2]_g,$$

where,

$$lnK_0 = 93.4517\left(\frac{100}{T}\right) - 60.2409 + 23.3585\ln\left(\frac{T}{100}\right),$$

where T is absolute temperature in K. In the flow cell system, where a more concentrated salt electrolyte is used, the effect of ionic strength on CO_2 solubility is considered. The presence of ions with high concentration decreases the solubility of CO_2 in solutions according to the Séchenov Equation:[5]

$$\log\left(\frac{[CO_2]_{aq,0}}{[CO_2]_{aq}}\right) = K_s C_s,$$

where,

$$K_s = \sum(h_{ion} + h_G)$$

$$h_G = h_{G,0} + h_T(T - 298.15)$$

Chemical and electrochemical reactions

The reaction rates of the following chemical equilibria are taken into consideration:

$$CO_2 + H_2O \overset{k_1, k_{-1}}{\leftrightarrow} H^+ + HCO_3^-$$

$$HCO_3^- \overset{k_2, k_{-2}}{\leftrightarrow} H^+ + CO_3^{2-}$$

$$CO_2 + OH^- \overset{k_3, k_{-3}}{\leftrightarrow} HCO_3^-$$

$$HCO_3^- + OH^- \overset{k_4, k_{-4}}{\leftrightarrow} CO_3^{2-} + H_2O$$

$$HSO_4^- \overset{k_5, k_{-5}}{\leftrightarrow} H^+ + SO_4^{2-}$$

$$H_2O \overset{k_w, k_{-w}}{\leftrightarrow} H^+ + OH^-$$

$$R_{CO_2} = -k_1[CO_2] + k_{-1}[H^+][HCO_3^-] - k_3[CO_2][OH^-] + k_{-3}[HCO_3^-]$$

$$R_{HCO_3^-} = k_1[CO_2] - k_{-1}[H^+][HCO_3^-] - k_2[HCO_3^-] + k_{-2}[H^+][CO_3^{2-}] + k_3[CO_2][OH^-] - k_{-3}[OH^-] + k_{-4}[CO_3^{2-}]$$

$$R_{CO_3^{2-}} = k_2[HCO_3^-] - k_{-2}[H^+][CO_3^{2-}] + k_4[HCO_3^-][OH^-] - k_{-4}[CO_3^{2-}]$$

$$R_{OH^-} = -k_3[CO_2][OH^-] + k_{-3}[HCO_3^-] - k_4[HCO_3^-][OH^-] + k_{-4}[CO_3^{2-}] + k_W - k_{-W}[H^+][OH^-]$$

$$R_{H^+} = k_1[CO_2] - k_{-1}[H^+][HCO_3^-] + k_2[HCO_3^-] - k_{-2}[H^+][CO_3^{2-}] + k_W - k_{-W}[H^+][OH^-] - [H^+][SO_4^{2-}]$$

$$R_{SO_4^{2-}} = k_5[HSO_4^-] - k_{-5}[H^+][SO_4^{2-}]$$

$$R_{HSO_4^-} = -k_5[HSO_4^-] + k_{-5}[H^+][SO_4^{2-}]$$

The CO_2 reduction and OH^- evolution happen on the left boundary (the electrode surface) in the planar electrode system:

$$R_{CO_2RR} = \frac{j}{nF},$$
$$R_{OHER} = -\frac{j}{F},$$

where j is the current density applied, F is Faraday's constant, and L_{CL} is the thickness of the catalyst layer, n is the number of electrons required for the reduction reaction, which is 2 for the CO production. In the flow cell system, CO_2 reduction and OH^- evolution happen uniformly at the CL domain:

$$R_{CO_2RR} = \frac{j}{n L_{CL} F},$$
$$R_{OHER} = -\frac{j}{L_{CL} F},$$

where L_{CL} is the thickness of the catalyst layer.

Liquid-phase transport

Transport of aqueous species is described via

$$\frac{\partial c_i}{\partial t} + \frac{\partial J_i}{\partial x} = R_i,$$

where J_i is the molar flux, given by:

$$J_i = -\frac{D_i \partial c_i}{\partial x},$$

where D_i is the diffusion coefficient of species i:

The effective diffusivity in the porous layer was corrected with porosity and tortuosity using the Bruggeman relationship:[3]

$$D_{e,i} = \frac{\varepsilon}{\tau} D_i = \varepsilon^{3/2} D_i$$

CO_2 dissolution

Gas-phase CO_2 dissolves into the electrolyte at the gas/liquid interface. In fully wetted GDE, gas/liquid interface only exists at the left boundary (corresponding to the interface of GDL and CL), where CO_2 is dissolved. In partially wetted GDE, both gas and liquid phases exist in CL. A thin film, with thickness δ_{TF}, covers the pore walls in the CL. It is derived from geometric parameters based on the CL saturation, S, by evenly distributing the electrolyte through pores of CL,

$$\delta_{TF} = r_{p,CL}(1 - \sqrt{1 - S}),$$

where $r_{p,CL}$ is the mean CL pore radius, assumed as 500 nm here.

The gas-to-liquid mass-transfer coefficient, k_{GL,CO_2}, is dependent on δ_{TF} and the diffusivity of CO_2 in liquid phase, D_{CO_2},

$$k_{GL,CO_2} = \frac{D_{CO_2}}{\delta_{TF}}$$

The dissolution of CO_2 can thus happen at the gas/liquid interface inside CL. The rate of CO_2 dissolution, R_{PT,CO_2}, contributes to the source term for CO_2,

$$R_{PT,CO_2} = a_v k_{GL,CO_2} M_{CO_2} (H_{CO_2} p_G y_{CO_2} - c_{CO_2(aq)})$$

where H_{CO_2} is Henry's constant for CO_2; p_G is the pressure of gas, which is 1 atm; y_{CO_2} is the mole fraction of CO_2 in gas phase, which is near unity under pure CO_2 supply; $c_{CO_2(aq)}$ is the dissolved CO_2 concentration.

Boundary conditions

The concentrations of aqueous species are set to be their bulk value at the right boundary. The aqueous species flux is set to zero at the left boundary. Additional left boundary conditions were set in GDE models: the mole fraction of gaseous CO_2 was set to be near unity (99.9%) at the left boundary.

Supplementary Figures

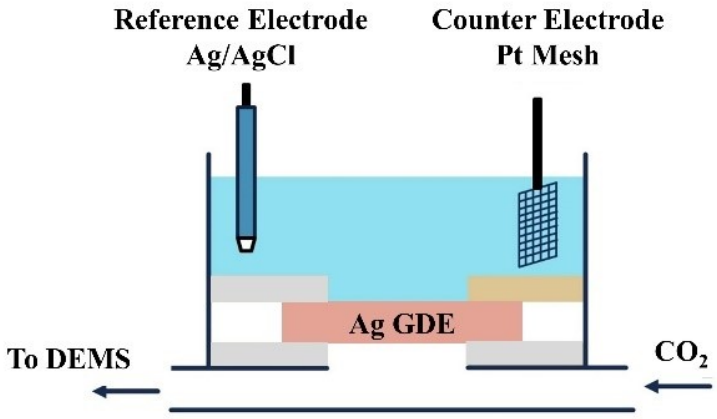

Supplementary Schematic 1. Schematic of gaseous products detection by SECM.

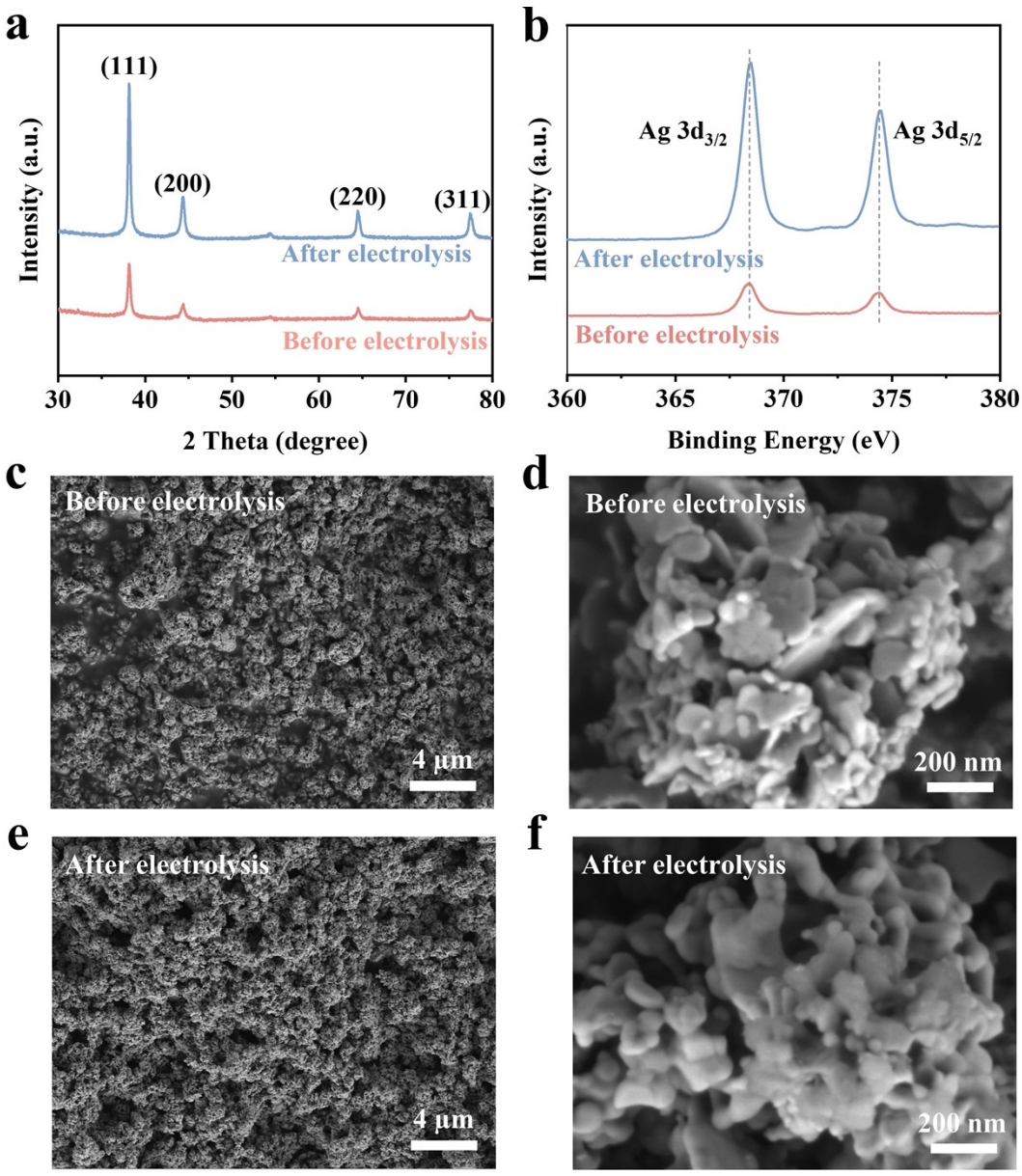

Supplementary Figure 1. X-ray diffraction patterns (a) and X-ray photoelectron spectroscopy (b) of Ag electrode before and after electrolysis. (c-d) Scanning Electrode Microscope (SEM) images of Ag electrode before electrolysis under different magnifications. (e-f) SEM images of Ag electrode after electrolysis under different magnifications. The electrolysis was performed under -100 mA cm^{-2} for 1 h in 0.5 M K_2SO_4 (pH = 2).

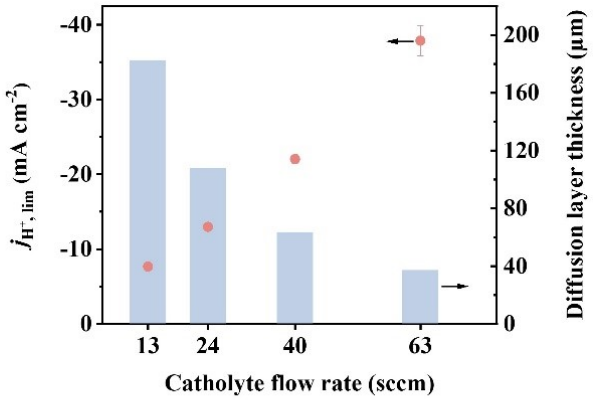

Supplementary Figure 2. Diffusion layer thickness of proton under different electrolyte flow rates, determined by the method mentioned in Supplementary Note 1. Error bars are means ± standard deviation (n = 3 replicates).

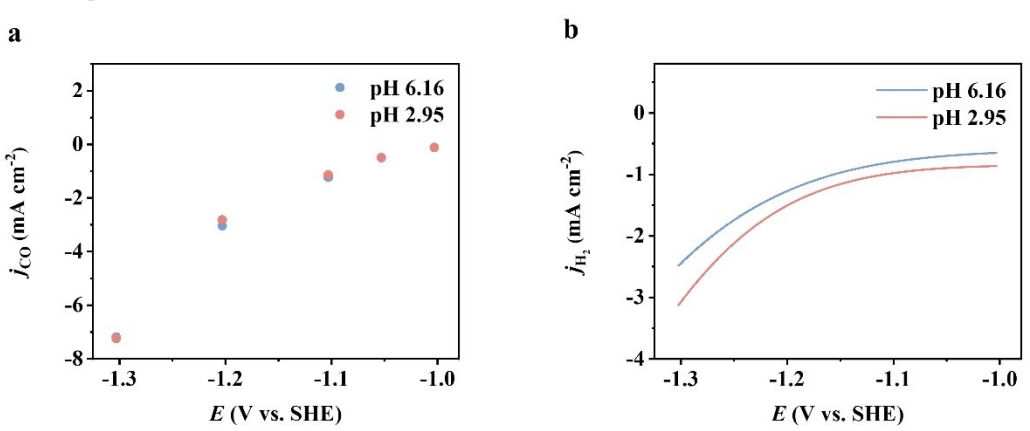

Supplementary Figure 3. a, Current density for CO production at various potentials under electrolytes with two different pH. **b,** current density for H_2 production at various potentials under electrolytes with two different pH. Error bars are means ± standard deviation (n = 3 replicates).

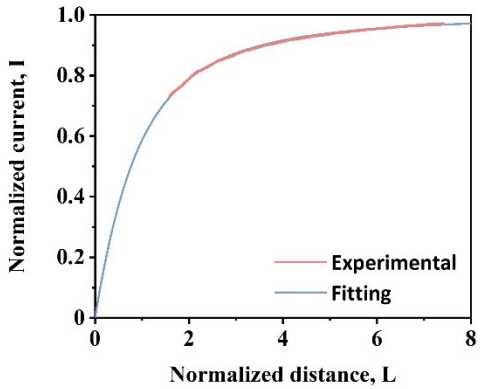

Supplementary Figure 4. Experimental and simulated approach curve of Pt UME via oxygen reduction reaction (ORR) method. The normalized distance, L, is *d*/*a*, where *d* is the tip-substrate distance and *a* is the radius tip. The normalized current is the tip current divided by the steady-state current at far away from the substrate.

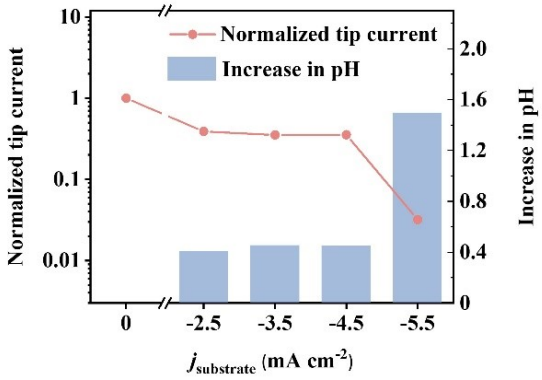

Supplementary Figure 5. The normalized tip HER-diffusion-limited current (DLC) at 50 μm away from the substrate, under different substrate applied current density at steady states, and the calculated increase in pH.

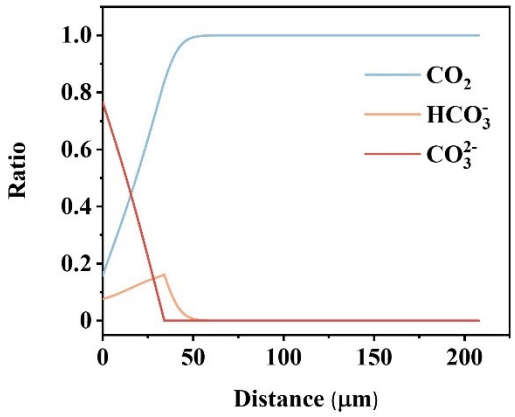

Supplementary Figure 6. The simulated ratio of different C species in total C within the diffusion layer, under -5.5 mA cm^{-2} applied current density.

Supplementary Tables

Supplementary Table 1. Séchenov constants

Ion	h_{ion}
K^+	0.0922
OH^-	0.0839
HCO_3^-	0.0967
CO_3^{2-}	0.1423
SO_4^{2-}	0.1117
Other parameters	
$h_{G,0}$	-0.0172
h_T	-0.000338

Supplementary Table 2. Rate constants for the reactions

k_1	$4.00 \times 10^{-2}\ s^{-1}$
k_{-1}	$93769.15\ L\ mol^{-1}\ s^{-1}$
k_2	$56.281\ s^{-1}$
k_{-2}	$1.23 \times 10^{12}\ L\ mol^{-1}\ s^{-1}$
k_3	$2.10 \times 10^{3}\ L\ mol^{-1}\ s^{-1}$
k_{-3}	$4.92 \times 10^{-5}\ s^{-1}$
k_4	$6.50 \times 10^{9}\ L\ mol^{-1}\ s^{-1}$
k_{-4}	$1.34 \times 10^{6}\ s^{-1}$
k_5	$2.50 \times 10^{9}\ s^{-1}$
k_{-5}	$3.00 \times 10^{10}\ L\ mol^{-1}\ s^{-1}$
k_w	$1.60 \times 10^{-3}\ mol\ L^{-1}\ s^{-1}$
k_{-w}	$1.60 \times 10^{11}\ L\ mol^{-1}\ s^{-1}$

Supplementary Table 3. Diffusion coefficient of the species

Species	Diffusion coefficient ($10^{-9} m^2 s^{-1}$)
CO_2	1.91
HCO_3^-	1.185
CO_3^{2-}	0.923
H^+	9.31
OH^-	5.293
HSO_4^-	1.39
SO_4^{2-}	1.07

Supplementary Table 4. Reynold's number at different electrolyte flow rate in a flow cell

Electrolyte flow rate (sccm)	Reynold's number
13	14
24	26
40	44
63	69

The calculation of Reynold's number is based on $Re = \frac{\rho Q D}{\mu A}$, where ρ is the density of water, 997 kg m^{-3}; Q is the experimentally measured flow rate of the electrolyte; μ is the viscosity of water, $1.01 \times 10^{-3} Pa\,s$; D is the diameter of flow cell chamber, which is 2 cm; A is the cross-sectional area of the flow cell chamber, which is 3 cm^2.

Supplementary References

[1] R. G. Compton, C. E. Banks, *Understanding voltammetry*, World Scientific, **2018**.
[2] D.-J. Chen, R. W. Penhallurick, Y. J. Tong, *J. Electroanal. Chem.* **2020**, *875*, 113918.
[3] L. C. Weng, A. T. Bell, A. Z. Weber, *Phys. Chem. Chem. Phys.* **2018**, *20*, 16973-16984.
[4] D. A. Wiesenburg, N. L. Guinasso, Jr., *J. Chem. Eng. Data* **1979**, *24*, 356-360.
[5] S. Weisenberger, A. Schumpe, *Aiche J.* **1996**, *42*, 298-300.